MOEM

Modern Electronic Materials 5(1): 13–19
DOI 10.3897/j.moem.5.1.46413

Research Article

Effect of proton doping and heat treatment on the structure of single crystal silicon

Victor E. Asadchikov[1], Irina G. Dyachkova[1], Denis A. Zolotov[1], Yuri S. Krivonosov[1], Vladimir T. Bublik[2], Alexander I. Shikhov[3]

1 *Shubnikov Institute of Crystallography of Federal Scientific Research Centre «Crystallography and Photonics» of Russian Academy of Sciences, 59 Leninsky Prospekt, Moscow 119333, Russia*

2 *National University of Science and Technology MISiS, 4 Leninsky Prospekt, Moscow 119049, Russia*

3 *HSE Tikhonov Moscow Institute of Electronics and Mathematics, 34 Tallinskaya Str., Moscow 123458, Russia*

Corresponding author: *Irina G. Dyachkova* (sig74@mail.ru)

Received 11 December 2018 ♦ **Accepted** 18 January 2019 ♦ **Published** 1 March 2019

Citation: Asadchikov VE, Dyachkova IG, Zolotov DA, Krivonosov YuS, Bublik VT, Shikhov AI (2019) Effect of proton doping and heat treatment on the structure of single crystal silicon. Modern Electronic Materials 5(1): 13–19. 10.3897/j.moem.5.1.46413

Abstract

The quality and structural perfection of single crystal silicon have been studied using double-crystal X-ray diffraction after hydrogen ion implantation and thermal annealing used in a number of semiconductor technologies. The fundamental difference of this approach is the possibility to rapidly obtain reliable experimental results which were confirmed using X-ray topography. Data have been presented for the condition of the damaged layer in *n*-type silicon single crystals (ρ = 100 $\Omega \times$ cm) having the (111) orientation and a thickness of 2 mm after proton implantation at energies E = 200, 300 and 100 + 200 + 300 keV and dose $D = 2 \times 10^{16}$ cm^{-2} and subsequent heat treatment in the T = 100–900 °C range. Using the method of integral characteristics we have revealed a nonmonotonic dependence of the integral characteristics of the damaged layer, i.e., the mean effective thickness L_{eff} and the mean relative deformation $\Delta a/a$, on the annealing temperature, the maximum deformation being observed for ~300 °C. The results have allowed us to make a general assessment of the damaged layer condition after heat treatment.

Keywords

silicon, implantation, thermal annealing, X-ray diffraction, X-ray topography, method of integral characteristics

1. Introduction

The investigations that have been carried out in recent years have shown the good promise of silicon irradiation with light ions (e.g. hydrogen and helium) for providing specific properties of the material that are unattainable with conventional methods [1–3]. This processing of silicon is promising for the development of a number of semiconductor technologies, including, for example, the formation of *p*–*i*–*n* photodiodes with improved parameters [4]. Earlier studies [5–8] some of which were carried out by the Authors [9–14] led to the conclusion that one of the main advantages of proton implantation into silicon is the capability to produce the so-called damaged layers. An important feature of these layers is the large number of structural defects generated by proton implantation and

© 2019 National University of Science and Technology MISiS. This is an open access article distributed under the terms of the Creative Commons Attribution License (CC-BY 4.0), which permits unrestricted use, distribution, and reproduction in any medium, provided the original author and source are credited.

during subsequent heat treatment. Depending on implantation mode and annealing temperature and time one can produce regions saturated with different types of defects:

- radiation-induced point defect clusters (eliminable by subsequent heat treatment);
- agglomerations of defects and hydrogen-filled micropores retained in the crystal after heat treatment;
- large hydrogen bubbles causing crystal surface erosion showing itself in superficial layer exfoliation at a depth of about the projection range of the implanted particles (protons in the case considered).

The presence of each of the structural defect types listed above can be used in specific semiconductor processes [1, 3, 4].

Currently there are several trends in the practical use of the properties of damaged layers generated by proton implantation and subsequent heat treatment:

- gettering of recombination impurities;
- separation of diffusion-bonded *n*- and *p*-type silicon wafers (the smart-cut technology);
- increasing the adhesion of films deposited onto silicon wafers;
- increasing the efficiency of photo-converters.

The aim of this work was to study the structural changes occurring in silicon single crystals as a result of ion implantation and to clarify their dependence on subsequent heat treatment. The aim of this work was achieved using the methods of double-crystal X-ray diffraction and X-ray topography. The results showed that double-crystal X-ray diffraction is sensitive to the defects forming as a result of ion implantation and subsequent heat treatment and is an efficient tool for rapid analysis of defect-containing structures. The experimental results were confirmed using X-ray topography. The information on the structure of ion-implanted specimens obtained in this work is helpful in the selection of the optimum ion implantation mode and post-implantation annealing temperature with the aim of increasing the quality and yield of devices.

2. Experimental

The specimens for the study were provided by Sapfir Co., Moscow, and were in the form of BDM-(AV) Grade single crystal silicon wafers which are used e.g. for the fabrication of *p–i–n* photodiodes. The Si wafers were *n*-type silicon single crystals ($\rho = 100\ \Omega \times$ cm) having the (111) orientation. The irradiation modes were as follows: proton energy E = 200 and 300 keV, the implantation dose being $D = 2 \times 10^{16}$ cm^{-2}. Some of the specimens were subjected to sequential irradiation with protons having different energies: 100 + 200 + 300 keV, the total dose being 2×10^{16} cm^{-2}. The specimens were irradiated at room temperature on an experimental implantation unit on the basis of a KT-500 cascade accelerator at the Research Institute for Nuclear Physics of the Moscow State University [15]. The proton current density was within 1 μA/cm^2 which avoided crystal heating to > 50 °C.

The results of preliminary irradiation of final-product semiconductor structures at Sapfir Co. showed that the device parameters for the as-proton irradiated silicon specimens (without heat treatment) were unstable. Earlier reports showed the good efficiency of irradiating the peripheral regions of n^+–p junctions with protons for protecting the surface of *p–i–n* photodiodes and correcting their characteristics with the aim to minimize the dark currents of photosensitive pads and guard rings [16]. We studied the behavior of the damaged layers after heat treatment in order to elaborate methods of increasing the stability of the devices and correcting the electrophysical parameters related to the increasing influence of the damaged layer. The as-irradiated specimens were vacuum-annealed in several stages at 100 to 900 °C with 50 °C steps for 2 h at each stage. The shortest annealing time was chosen based on the sensitivity of the X-ray diffraction method used for studying the structure of the damaged layer. An increase in the annealing duration did not change significantly the condition of the damaged layer for each specific annealing temperature.

The choice of implantation dose is dictated by the necessity of obtaining a layer containing the maximum number of imperfections and possessing stable properties. It was demonstrated [17] that an increase in the dose to above 2×10^{16} cm^{-2} causes the formation of gas bubbles and destruction of silicon single crystals during subsequent heat treatment.

The energy of the implanted protons is selected with the aim to generate a damaged layer at depths comparable with the *p–n* junction location depth in industrial devices (approx. 2 μm).

The depth profiles of the implanted hydrogen ions and the radiation-induced defects in the irradiated silicon single crystals (Fig. 1) for 100, 200 and 300 keV irradiation energies were analyzed using the Pearson method [18] with the TRIM software (Transport of Ions in Matter) [19]. It can be seen from Fig. 1 that the location of the concentration peaks in the impurity and radiation-induced defect depth profiles were almost the same for similar implantation energy and agree with the projection range of protons having the respective energy. However, the calculated point defect concentrations proved to be higher than the hydrogen concentration, the difference being 1.4 times for 100 keV implantation and 1.7 times for 300 keV implantation. The Monte–Carlo radiation defect profiles have well-pronounced bell shapes shifting to greater depths with an increase in energy [18]. The profile width increases with the energy of the ions, while the height of the concentration peak decreases. However, the overall curve area suggests an increase in the total number of defects generated by one ion.

Thus, sequential implantation of the specimen with ions at energies increasing stepwise from 100 to 300 keV

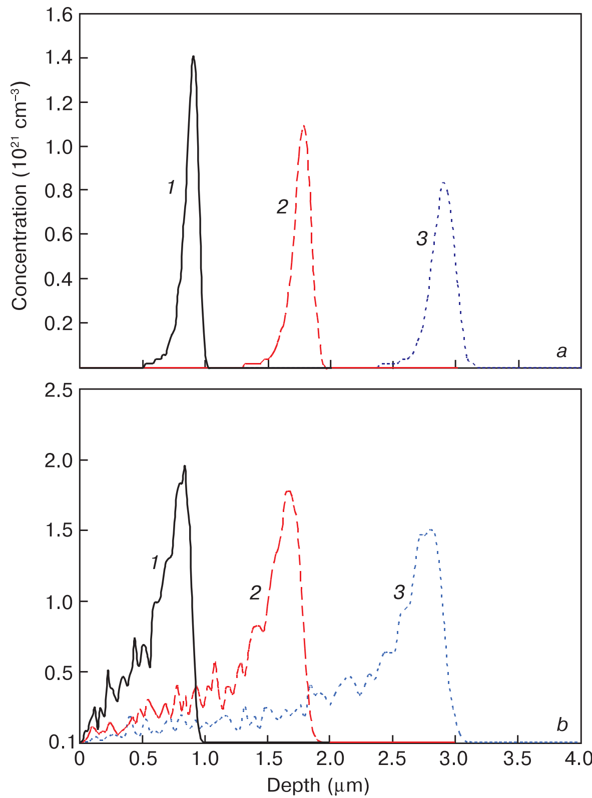

Figure 1. (*a*) Implanted hydrogen and (*b*) radiation defect profiles in Si specimen calculated by TRIM software for implantation at (*1*) 100, (*2*) 200 and (*3*) 300 keV energies.

allows producing a quasi-uniform, depth-smeared damaged layer the width of which is greater compared with that for implantation at a single energy. Aimed at solving practical tasks and increasing the sensitivity of the X-ray diffraction and X-ray topography structural study methods we implanted one of the specimens sequentially with hydrogen ions at energies $E = 100 + 200 + 300$ keV. The diffraction reflection curve of the initial specimen and the rocking curves, i.e., the angular dependences of reflection intensity from the crystal, for all the abovementioned implantation and annealing modes were taken on an X-ray diffractometer in the (n, $-n$) double-crystal setup. The X-ray diffraction pattern provides information on the imperfections in the crystalline structure of the specimens at the depth corresponding to the X-ray extinction length L_{ext}; one can see changes in the interplane spacing and the atomic disorder degree with increasing depth. Therefore in order to increase the extinction length ($L_{ext} \approx 8.03$ μm in the case considered) we used the third-order (111) plane reflection for Cu$K_{\alpha 1}$ radiation ($\lambda = 0.1541$ nm).

For the measurements we took the “all at maximum” position as the zero point corresponding to the reciprocal lattice site for the reflection used. A 1 mm slot was provided in front of the detector for precision Bragg reflection adjustment. The slot was later removed for rocking curve measurement. The source beam was collimated with a 0.1 mm horizontal slot and a 12 mm vertical slot. The diffraction reflection curves of the initial silicon single crystal were taken by automatic crystal rotation in the –25” to +25” angle range around the diffraction angle ($\theta_B = 47.5$ arc deg) with a 0.1” angle step. The rocking curves of the as-implanted and as-annealed silicon single crystals were taken by automatic crystal rotation in the –90” to +30” angle range around the diffraction angle with a 0.5” angle step. The pulse gain time was 1 to 100 s per point and at least 100 s for statistical data accumulation. These data were used for further calculation of the mean effective thickness L_{eff} and the mean relative deformation $\Delta a/a$ using the method of integral characteristics [20]. The principle underlying the method of integral characteristics is as follows.

The difference between the total areas under the rocking curve of a crystal having a damaged layer and the rocking curve of a perfect crystal can be written in the following form [20]

$$\Delta S^{(0)} = \frac{1}{\pi}\int_{-\infty}^{\infty}\frac{\left[P_R(\theta) - P_R^0(\theta)\right]\mathrm{d}\theta}{\theta_0} = \frac{1}{L_{ext}}\int_0^{\infty}\left\{\exp\left[-2w(z)\right] - \exp\left[-w(z)\right]\cos\left(K_h u(z)\right)\right\}\mathrm{d}z, \quad (1)$$

where $P_R(\theta)$ is the intensity of scattering by the layer/substrate system (hereinafter the substrate will be considered as the undamaged silicon structure region), $P_R^0(\theta)$ is the intensity of scattering from the substrate, θ_0 is the width of the diffraction reflection curve, L_{ext} is the extinction depth, $w(z)$ is the Debye-Waller factor describing the random movements of atoms around their positions in the perfect lattice (physically $\exp(-w(z))$ describes the amorphization degree of the damaged layer caused by various defects forming during the implantation), K_h is the diffraction vector, and $u(z)$ is the displacement of the atomic planes in the damaged layer relative to their respective positions in the substrate.

At relatively large $u(z)$, theoretical Eq. (1) transforms to the following simpler expression

$$\Delta S^{(0)} = \frac{1}{L_{ext}}\int_0^{L_1}\exp\left[-2w(z)\right]\mathrm{d}z \cong \frac{L_1}{L_{ext}}. \quad (2)$$

In other words, the parameter $\Delta S^{(0)}$ determines the thickness of the damaged layer. We write this expression for the first statistical moment of the experimental rocking curve:

$$\Delta S^{(1)} = \frac{2}{\pi\theta_0^2}\int_{-\infty}^{\infty}\left[P_R(\theta) - P_R^0(\theta)\right]\theta\mathrm{d}\theta = \int_0^{L_1}\Delta a(z)\exp\left[-w(z)\right]\mathrm{d}z, \quad (3)$$

where L_1 is the thickness of the damaged layer.

For low amorphization when exp(–$w(z)$) ≅ 1, the parameter $\Delta S^{(1)}$ determines the mean deviation of the crystalline lattice parameter of the damaged layer, i.e.,

$$\Delta S^{(1)} \approx \overline{\Delta a(z)}L_1. \quad (4)$$

The diffraction reflection curve of the initial silicon specimen is shown in Fig. 2, and the rocking curves of the as-irradiated and as-annealed specimens are presented in Fig. 3.

The half-width of the diffraction reflection curve of the initial silicon specimen before any treatment (Fig. 2) is ~3” which is in agreement with the calculated theoretical values [21]. Thus, the initial single crystal is highly perfect and contains a minimal quantity of defects.

The rocking curves of the as-irradiated specimens (Fig. 3) contain, along with the Bragg peak, an additional reflection intensity hill in its vicinity. The intensity of the additional reflection hill is not high, a few percents. However the angle range of the additional reflection intensity hill is large, hundreds of angle seconds. This scattering feature is caused by the formation of a thin damaged layer due to the radiation-induced defects near the surface of the irradiated single crystals. The lattice distortion in the layer changes the average interplane spacing Δa and produces X-ray beam reflections at angles differing from the exact Bragg angle.

Figure 4 shows a Lang X-ray section topography [22] image of the damaged layer generated by proton implantation into the surface layer of single crystal silicon. The image was obtained on a ROTAFLEXRU-200B instrument [15] in Mo$K_{\alpha 1}$ radiation, wavelength 0.07093 nm. The focus projection of the sharp-focused X-ray source was 0.4 × 0.4 mm². The ~10 μm wide ribbon-shaped beam was formed before the specimen with narrow vertical slots: one slot ~100 μm in width was at a 1.9 m distance from the specimen and the other slot ~10 μm in width was at a 0.25 m distance after the first slot. The position of the (111) single crystal silicon specimen was adjusted until a strong diffraction beam for the characteristic $K_{\alpha 1}$ line was obtained for the (133) diffraction plane (θ_B = 16.5 arc deg). Thus, a tilted reflection was used for increasing the size of the damaged layer image in the X-ray topographic pattern. Note that the angle between the (111) and (133) planes is ~22 arc deg providing for an increase in the detectable damaged layer thickness from 4 to 50 μm. The influence of the projection magnification due to the beam divergence at the distance between the specimen and the photographic plate is negligible. For our experiment we achieved a high spatial resolution by choosing the distance between the specimen and the photographic plate to be 40 mm for a 0.4 mm vertical focus projection located at 2300 mm from the specimen.

The size of the primary radiation-induced defects and complexes is small as compared with the resolution of X-ray topography and therefore they cannot be resolved individually. The damaged layer is seen in the X-ray topographic pattern as a dark band against the light background of the silicon matrix. Strictly speaking, the conditions under which the image shown in Fig. 4 was taken are not in full compliance with the section topographic pattern criteria since the width of the incident beam (~10 μm) is smaller than the crystal thickness (~400 μm) but appreciably greater than the damaged layer thickness (~3 μm). Topographic patterns taken under such conditions are not projection ones with regard the damaged layer. Yet they resolve a region of the maximum damage and the surface layer with a low defect concentration.

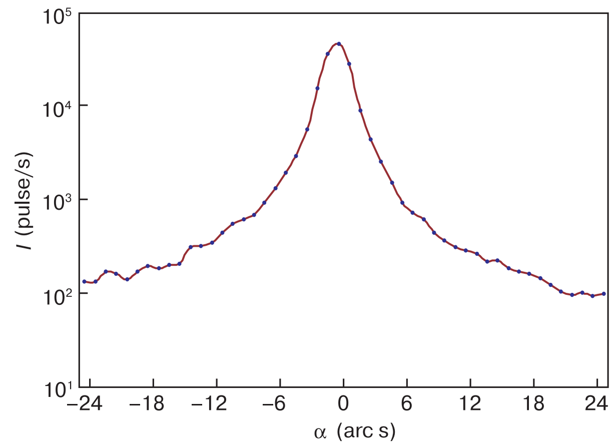

Figure 2. Diffraction reflection curve of the initial specimen.

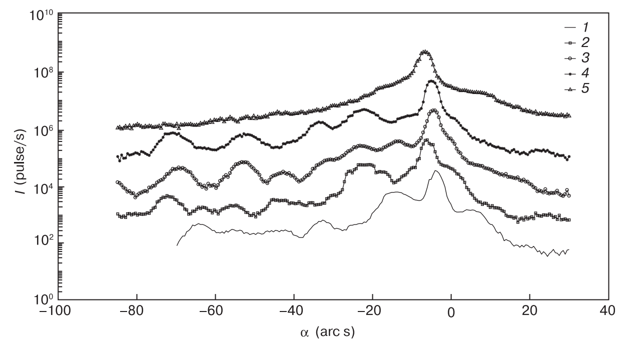

Figure 3. Rocking curves of silicon specimens irradiated with protons at E = 100 + 200 + 300 keV and D = 2 × 10^{16} cm^{-2} and annealed at different temperatures T, °C: (*1*) 0, (*2*) 200, (*3*) 250, (*4*) 300 and (*5*) 600.

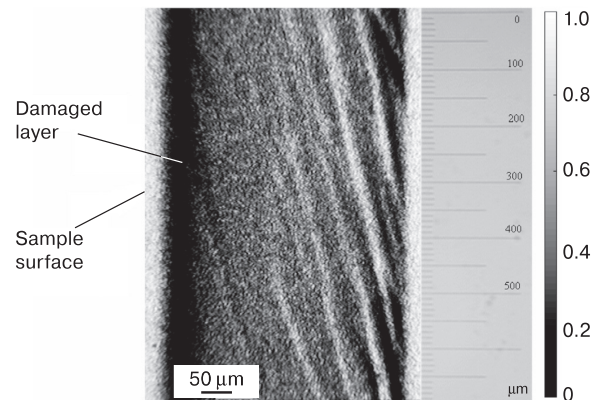

Figure 4. Section topographic image of damaged layer in silicon crystal irradiated with protons at E = 100 + 200 + 300 keV and D = 2 × 10^{16} cm^{-2}.

It is noteworthy that additional coherent oscillations can be seen in the rocking curves of the specimens predominantly at angles that are smaller than the Bragg angle (Fig. 3). This indicates an increase in the lattice parameter of the damaged layer. One can therefore assume that interstitial type defects give the main contribution to the lattice damage. Since the bombarding particle energy is typically imparted to the target atoms during implantation in the forward direction, interstitial atoms have a somewhat deeper profile than vacancies. This must therefore produce a vacancy-rich layer close to the specimen surface and a layer rich in interstitial atoms near the end of the ions' projection range. Interstitial atoms are known to distort the lattice stronger than vacancies, and therefore a superimposition of vacancy and interstitial solid solutions (as in the case considered) produces an increase in the lattice parameter; this was confirmed by the diffraction experiment [23]. Vacancy type defects show themselves in electrophysical experiments [24, 25].

Annealing at T = 300 °C produces an additional scattering region in the rocking curves of the specimens, the intensity of the reflection being even greater than for the as-irradiated specimens in which the additional scattering hill was already depleted almost completely after annealing at 600 °C (Fig. 3).

3. Results and discussion

We used the method of integral characteristics for the treatise of the experimental results [20]. This method only accounts for the integral intensity scattered in the vicinity of the diffraction maximum; this provides for the high speed of the method and the capability of consistent treatise of the results. For the processing of the results we developed a computer program for calculating the effective damaged layer thickness L_{eff} and the mean deformation in the layer $\Delta a/a$. The effective damaged layer thickness L_{eff} and the mean deformation $\Delta a/a$ of the damaged layer as a function of irradiation mode and annealing temperature are shown in Figs 5, 6, respectively. These data suggest that irradiation of the silicon single crystals at a 200 keV energy and a 2×10^{16} cm^{-2} dose gives L_{eff} that agrees with the proton projection range and reaches ~2.5 µm, while irradiation at 300 keV gives $L_{eff} \sim 3.2$ µm. After sequential irradiation with proton energy combination 100 + 200 + 300 keV L_{eff} increases to 4.5 µm. The mean deformation of the damaged layers exhibits a similar behavior as a function of irradiation energy.

The common feature of the experimental curves is a nonmonotonic change of the integral characteristics with an increase in temperature. Increasing the annealing temperature to 200 °C causes a linear decrease in L_{eff} for all the irradiation modes, but after T = 250 °C L_{eff} increases appreciably. Noteworthy, L_{eff} and $\Delta a/a$ increase for all the irradiation modes in the 200–300 °C range. One can assume that the transformation, re-association and rearrangement of radiation-induced defects caused by annealing in this temperature range lead to the formation

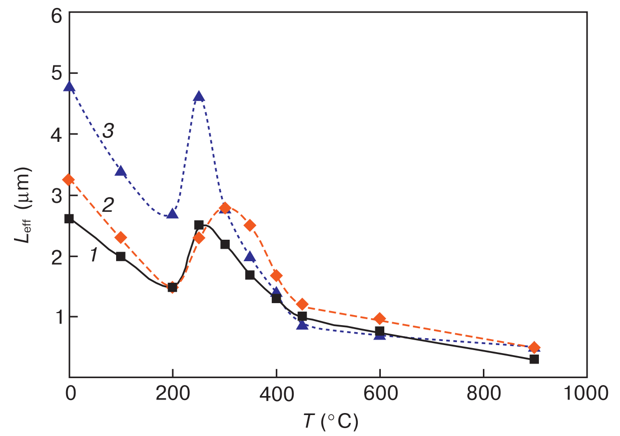

Figure 5. Effective damaged layer thickness in silicon specimens as a function of annealing temperature for proton implantation at energies E, keV: (*1*) 200; (*2*) 300; (*3*) 100 + 200 + 300.

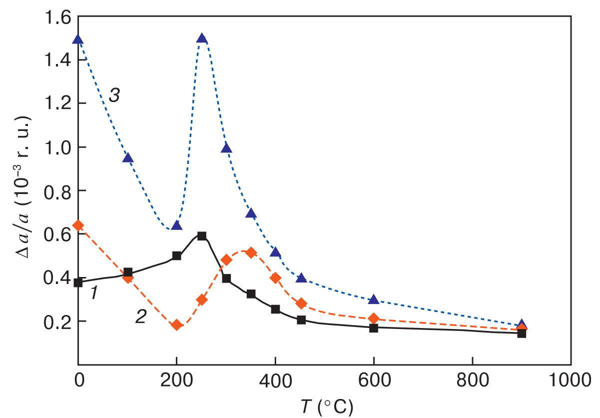

Figure 6. Mean relative deformation of damaged layer in silicon specimens as a function of annealing temperature for proton implantation at energies E, keV: (*1*) 200; (*2*) 300; (*3*) 100 + 200 + 300.

of complexes and clusters consisting of simple defects and interstitial hydrogen atoms. Another assumption is the formation of hydrogen-filled micropores. Possibly the composition of these microdefects produces an especially strong distortion in the damaged layer, causing an increase in the average values of the integral characteristics in all the cases considered above.

X-ray topography also revealed a nonmonotonic change in the thickness of the damaged layer with an increase in the annealing temperature. The X-ray section topographic pattern for the specimen annealed at 300 °C exhibits an increase in the thickness of the damaged layer compared with the as-irradiated specimen (Fig. 7*a*).

The X-ray topographic pattern for the specimen annealed at 300 °C (Fig. 7*a*) also exhibits a darker damaged layer as compared with the as-irradiated specimen (Fig. 4). (The specimens were topographed under the same conditions, and the photographic plates were developed simultaneously.) This seems to originate from an increase in the deformation in the damaged layer.

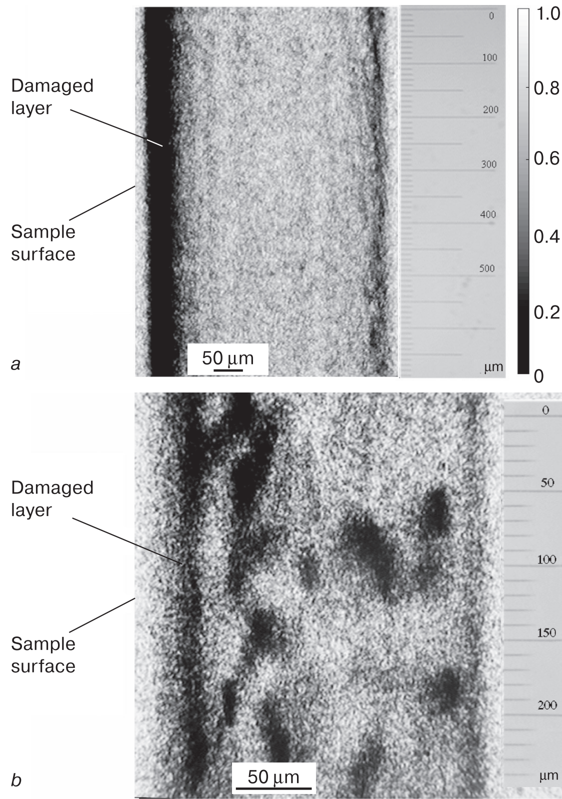

Figure 7. Section topographic image of damaged layer in silicon crystal irradiated with protons at E = 100 + 200 + 300 keV and $D = 2 \times 10^{16}$ cm^{-2} and annealed at T (*a*) 300 and (*b*) 900 °C.

Further increasing the annealing temperature to 400 °C changes L_{eff} in a specific manner for each of the irradiation modes. However, the L_{eff} and $\Delta a/a$ functions of annealing temperature exhibit a similar behavior in the entire annealing temperature range for each specific irradiation mode and different behaviors for different irradiation modes. For 200 and 300 keV irradiation energies the temperature dependence peaks (at T = 250–350 °C) are appreciably weaker and wider compared with irradiation at E = 100 + 200 + 300 keV and shifted towards higher temperatures. Increasing the annealing temperature from 400 to 900 °C is accompanied by a gradual decrease in the integral characteristics. At 900 °C the damage in the layer is but slight. This, however, does not indicate that microdefects are absent in the damaged layer. X-ray topography showed that 900 °C heat treatment actually anneals the surface layer of the crystal where the concentration of the radiation defects was initially lower than at the depth corresponding to the ions' projection range where the structure is not restored by annealing (Fig. 7*b*). The dark spots revealed in the depth of the crystal indicate the typical coagulation of oxygen precipitates during high-temperature annealing of Cz-grown silicon single crystals [23].

Double-crystal X-ray diffraction no longer detects the mean lattice deformation after annealing at above 500 °C. Point defect complexes, clusters and pores forming at these post-implantation annealing temperatures have a smaller influence on the lattice parameter of the crystal than the influence of unassociated point defects, and therefore the positive and negative lattice deformations generated by these defects are compensated.

4. Conclusion

The condition of the damaged layer in single crystal silicon was studied using double-crystal X-ray diffraction after proton implantation at E = 200, 300 and 100 + 200 + 300 keV and dose $D = 2 \times 10^{16}$ cm^{-2} and subsequent heat treatment in the 100 to 900 °C range. The integral characteristics of the damaged layer have a nonmonotonic dependence on the annealing temperature, the maximum damage being observed for ~300 °C.

The high-resolution double-crystal X-ray diffraction method proved to be sensitive to damaged layer condition. Combination of this experimental tool with data processing using the method of integral characteristics provides for rapid analysis of defect-containing structures aiming at elaboration of technologies for a number of semiconductor devices involving the introduction of radiation-induced defects.

Detailed analysis of oscillations observed in the diffraction reflection curves for the test specimens taken using triple-crystal X-ray diffraction combined with electron microscopy imaging will be published later.

Acknowledgements

The Authors are grateful to Nikolai V. Kuznetsov, Senior Researcher, Research Institute for Nuclear Physics of the Moscow State University, for irradiating the specimens at the KT-500 accelerator.

This work was supported by the Ministry of Science and Higher Education within the State assignment FSRC "Crystallography and Photonics" RAS.

References

1. Kozlovski V. V. *Modifitsirovanie poluprovodnikov puchkami protonov* [Modification of semiconductors by proton beams]. St. Petersburg: Nauka, 2003. 268 p. (In Russ.)
2. Smirnov I. S., Kuznetsov N. V., Soloviev G. G. Formation of layers with special properties in silicon by implantation of protons and heat treatment. *XVI Vsesoyuznaya konferentsiya po fizike vzaimodeistviya*

zaryazhennykh chastits s kristallom = XVI All-Union conference on physics of interaction of charged particles with crystal. Moscow: MGU, 1988, pp. 78–81. (In Russ.)

3. Bruel M. Silicon on insulator material technology. *Electronics Lett*. 1995, vol. 31, no. 14, pp. 1201–1202. https://doi.org/10.1049/el:19950805
4. Gubarev V., Semenov A., Surma A., Stolbunov V. Technology of proton irradiation and the possibility of its application to improve the characteristics of power diodes and thyristors. *Silovaya Elektronika.* 2011, no. 5, pp. 108–111. (In Russ.)
5. Smirnov I. S., Soloviev G. G., Novoselova E. G., Gurinov D. E. Formation of layers with special properties in silicon by implantation of protons and heat treatment. *VII Mezhnatsional'noe soveshchanie «Radiatsionnaya fizika tverdogo tela» = VII International Meeting «Radiation physics of solids»*. Moscow: MGIEM, 1997, pp. 230–231. (In Russ.)
6. Irmscher K., Klose H., Maass K. Hydrogen-related deep levels in proton-bombarded silicon. *J. Phys. C: Solid State Phys*., 1984, vol. 17, no. 35, pp. 6317–6329. https://doi.org/10.1088/0022-3719/17/35/007
7. Kirnstötter S.,Faccinelli M., Jelinek M., Schustereder W., Laven J. G., Schulze H. J., Hadley P. Multiple proton implantations into Silicon: A combined EBIC and SRP study. *Solid State Phenomena*, 2014, vol. 205–206, pp. 311–316. https://doi.org/10.4028/www.scientific.net/SSP.205-206.311
8. Bezrodnykh I. P., Tyutnev A. P., Semenov V. T. *Radiatsionnye effekty v kosmose. Chast' 3. Vliyanie ioniziruyushchego izlucheniya na izdeliya elektronnoi tekhniki* [Radiation effects in space. Pt 3. Influence of ionizing radiation on electronic products]. Moscow: AO «Korporatsiya «VNIIEM», 2017. 64 p. (In Russ.)
9. Dyachkova I. G., Novoselova E. G, Smirnov I. S. Implantation of a silicon wafer with protons under conditions of intense mechanical surface layer. *XXIV Mezhdunarodnaya konferentsiya «Radiatsionnaya fizika tverdogo tela» = XXIV International Conference «Radiation physics of solids»*. Moscow: FGBNU «NII PMT», 2014, pp. 512–518. (In Russ.)
10. Dyachkova I. G., Novoselova E. G., Smirnov I. S. Influence of temperature on the formation of disturbed layers in silicon under proton irradiation. *XXV Mezhdunarodnaya konferentsiya «Radiatsionnaya fizika tverdogo tela» = XXV International Conference «Radiation physics of solids».* Moscow: FGBNU «NII PMT», 2015, pp. 539–549. (In Russ.)
11. Smirnov I. S., Novoselova E. G., Dyachkova I. G. Influence of temperature on the formation of defects in silicon crystals during proton implantation. *Sed'moi mezhdunarodnyi nauchnyi seminar i Pyataya mezhdunarodnaya molodezhnaya nauchnaya shkola-seminar «Sovremennye metody analiza difraktsionnykh dannykh i aktual'nye problemy rentgenovskoi optiki» = The Seventh International Scientific Seminar and the Fifth International Youth Scientific School-seminar «Modern methods of the analysis of diffraction data and actual problems of x-ray optics»*. Velikiy Novgorod, 2015, pp. 222–225. (In Russ.)
12. Dyachkova I. G., Novoselova E. G., Smirnov I. S. Transformation of radiation defects in proton-implanted silicon during low-temperature heat treatment. *XXVI XXVI Mezhdunarodnaya konferentsiya «Radiatsionnaya fizika tverdogo tela» = XXVI International Conference «Radiation physics of solids».* Moscow: FGBNU «NII PMT», 2016, pp. 362–370. (In Russ.)
13. Dyachkova I. G., Novoselova E. G., Smirnov I. S., Monakhov I. S. Influence of mechanical stresses on defect formation in silicon under irradiation by protons. *12-ya Mezhdunarodnaya konferentsiya «Vzaimodeistvie izluchenii s tverdym telom» = 12th International Conference «Interaction of radiation with a solid body»*. Minsk, 2017, pp. 140–141. (In Russ.)
14. Dyachkova I. G., Novoselova E. G., Smirnov I. S. On the implantation of protons into silicon plates in the case of a mechanically stressed surface layer. *Journal of Surface Investigation: X-ray, Synchrotron and Neutron Techniques*, 2018, vol. 12, no. 3, pp. 613–618. https://doi.org/10.1134/S1027451018030278
15. Dyachkova I. G. The formation of damage layers in silicon crystals implanted with protons. Thesis of Cand. Sci. (Phys.-Math.). Moscow, 2004. 172 p. (In Russ.)
16. Sorokin K. V. Research and development of methods of surface protection of silicon photodiodes using ion implantation. Thesis of Cand. Sci. (Eng.). Moscow, 2000. 145 p. (In Russ.)
17. Aleksandrov P. A., Baranova E. K., Baranova I. V., Budaragin V. V., Litvinov V. L. The effect of annealing temperature on the output of implanted hydrogen blisters in silicon. *XII Mezhdunarodnoe soveshchanie «Radiatsionnaya fizika tverdogo tela» = XII International Conference «Radiation physics of solids»*. Moscow: NII PMT MGIEM (TU), 2002, pp. 149–160. (In Russ.)
18. Burenkov A. F., Komarov F. F., Kumakhov M. A., Temkin M. M. *Tablitsy parametrov prostranstvennogo raspredeleniya ionno-implantirovannykh primesei* [Tables of parameters of the spatial distribution of ion-implanted impurities]. Minsk: BGU, 1980. 352 p. (In Russ.)
19. Posselt M. Crystal-TRIM and its application to investigations on channeling effects during ion implantation. *Rad. Eff. Defects in Solids*, 1994, no. 1, pp. 87–119. https://doi.org/10.1080/10420159408219774
20. Afanas'ev A. M., Aleksandrov P. A., Imamov R. M. *Rentgenodifraktsionnaya diagnostika submikronnykh sloev* [X-ray diffraction diagnostics of submicron layers]. Moscow: Nauka, 1989. 152 p. (In Russ.)
21. Pinsker Z. G. *Dinamicheskoe rasseyanie rentgenovskikh luchei v ideal'nykh kristallakh* [Dynamical scattering of x-rays in perfect crystals]. Moscow: Nauka, 1974. 368 p. (In Russ.)
22. Bowen D. K., Tanner B. K. *Vysokorazreshayushchaya rentgenovskaya difraktometriya i topografiya* [High resolution x-ray diffractometry and topography]. St. Petersburg: Nauka, 2002. 274 p. (In Russ.)
23. Vavilov V. S., Kiselev V. F., Mukashev B. N. *Defekty v kremnii i na ego poverkhnosti* [Defects in silicon and on its surface]. Moscow: Nauka, 1990. 216 p. (In Russ.)
24. Grekhov I. V., Kostina L. S., Lomazow V. N., Yusupova S. A., Belyakova E. I. Formation of distribution profiles of small donors during proton irradiation of silicon. *Pis'ma v zhurnal tekhnicheskoi fiziki = Tech. Phys. Lett.*, 2014, vol. 40, no. 23, pp. 67–73. (In Russ.) https://doi.org/10.1134/S1063785014120086
25. Emtsev V. V., Ivanov A. M., Lebedev A. A., Oganesyan G. A., Strokan N. B., Kozlovskii V. V. Comparative study of changes in electrical properties of silicon and silicon carbide upon proton irradiation. Semiconductors, 2010, vol. 44, no. 5, pp. 678–684. https://doi.org/10.1134/S1063782610050234